Spectroscopic and theoretical studies of the excited states of fenofibric acid and ketoprofen in relation with their photosensitizing properties†

Virginie Lhiaubet,[a] Fabien Gutierrez,[b] Florence Penaud–Berruyer,[c] Edmond Amouyal,[c] Jean-Pierre Daudey,[b] Romuald Poteau,[b] Nadia Chouini–Lalanne[a] and Nicole Paillous*[a]

[a] *Laboratoire des Interactions Moléculaires et Réactivité Chimique et Photochimique (CNRS UMR 5623), Université Paul Sabatier, 118 route de Narbonne, 31062 Toulouse cedex 4, France. E-mail: paillous@ramses.ups-tlse.fr; Fax: +33 5 61 25 17 33*

[b] *Laboratoire de Physique Quantique (CNRS UMR 5626), IRSAMC, Université Paul Sabatier, 118 route de Narbonne, 31062 Toulouse cedex 4, France*

[c] *Laboratoire de Physicochimie des Rayonnements, Université Paris-Sud, Bat 350, 91450 Orsay cedex, France*

Received (in Montpellier, France) 1st December 1999, Accepted 10th March 2000
Published on the Web 5th May 2000

A study of the different excited states of fenofibric acid (FB) and ketoprofen (KP), two aromatic acids derived from benzophenone, has been achieved by absorbance and low temperature emission spectroscopy to take into account their photochemical reactivity and their *in vitro* and *in vivo* photosensitizing properties. These experiments have shown that FB mainly exhibits a singlet-singlet transition of $\pi\pi^*$ character, the $n\pi^*$ transition being undetectable, in contrast with KP. In phosphate buffer as well as in ethanol or in isopentane, the lowest triplet excited state of fenofibric acid appears to be, as for KP, an $n\pi^*$ triplet state with characteristics similar to those of benzophenone. These assignments were fairly well supported by theoretical calculations performed at the TD-DFT level. The transient formation of a ketyl radical detected in flash photolysis experiments performed in ethanol confirms that the photochemical reactivity of FB towards hydrogen abstraction in ethanol is typically that of an $n\pi^*$ triplet state. The good agreement between the experimental and theoretical results is discussed with respect to those previously obtained by other theoretical methods.

Elucidating of the action mechanism of phototoxic drugs is a challenge that has led photochemists to revisit the behaviour of classical photosensitizers.[1] This may be illustrated by the present study on fenofibric acid (FB), the main metabolite of fenofibrate, a hypolipidemiant agent, and ketoprofen (KP), a nonsteroidal antiinflammatory drug (NSAID), which both contain a benzophenone chromophore.[2] Both drugs induce photoallergic contact dermatitis and promote photocrossreactions with benzophenone (BP), a well known photosensitizer,[3] providing evidence that their photosensitizing properties are directly correlated to the presence of the carbonyl group. However, it should be noted that cutaneous photosensitivity due to KP, which may also include phototoxic effects,[4–9] is more frequently mentioned than that of FB.[4,5,10]

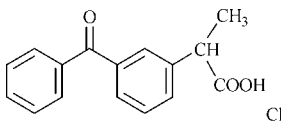

Ketoprofen (KP)

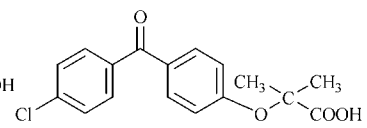

Fenofibric Acid (FB)

Previous studies have shown that *in vitro*, the photolysis of both compounds goes through two pathways: a photopinacolization occurring in alcohols,[11,12] which is one of the most widely studied photoreactions of benzophenone derivatives, and a (preponderant) photodecarboxylation taking place in phosphate buffer, usually observed with NSAID propionic acid derivatives.[13–15] However, the photoreactivity of FB in phosphate buffer is clearly lower than that of KP, as is its efficiency to photosensitize DNA cleavage.[16] The photodecarboxylation of both drugs is assumed to occur through an ionic pathway with the transient formation of a carbanion, which is a very unusual process in photochemistry. The ionic character of the decarboxylation process of KP has been associated either to a short-lived triplet excited state with a pronounced $\pi\pi^*$ character[17] or possibly a $\pi\pi^*$ singlet state.[18] To clarify this controversial point, it was judged useful to obtain clear assignments on the nature of the excited states of FB and KP involved in the primary processes of these reactions. The aim of this work was to establish a state energy diagram of the excited states of these drugs and of BP in order to gain insight into their photochemical reactivity. These investigations were carried out by absorption and emission spectroscopy on FB and KP and the data compared to previous results obtained with BP. Flash photolysis experiments were undertaken to examine the photoreactivity of FB in ethanol and to confirm the nature of the lowest excited states involved.

Theoretical calculations were also performed and the calculated spectra were compared to those obtained experimentally. Although quantum chemical methods have been applied with success to study the properties of rather large molecules in their ground electronic state, the computation of excited states is a more difficult task, due to the crucial role of electronic correlation. It should be emphasized that while BP has been extensively studied, a complete state energy diagram could not be found in the literature. The lowest singlet and triplet excited states of BP are relatively well documented but the localisation of the higher excited states remains largely controversial.[19–21] So, the computation of the excited states of these three compounds was a real challenge, even for BP.

† *Non-SI unit employed:* 1 kcal $mol^{-1} \approx 4.18$ kJ mol^{-1}.

As a matter of fact, there are only a few theoretical methods able to provide a quantitative or even qualitative description of the excited states of large molecules. For example, the errors with the *ab initio* CASPT2 method,[22] which is often considered as yielding the most accurate transition energies, are in the range 0–7 kcal mol^{-1}. However, at the present time, this method cannot be applied to large systems such as KP or FB.

Time-dependent density functional theory (TD-DFT), which is an interesting alternative to the *ab initio* CI or semi-empirical methods, was chosen to investigate the electronic properties of BP, KP and FB (for reviews, see ref. 23). DFT is known to provide accurate results for the electronic ground state of a wide variety of molecules. Its time-dependent formulation describes the dynamic response of the charge density, and allows the calculation of vertical electronic excitation spectra, since it yields dipole-allowed and dipole-forbidden transitions. It has been recently applied with success to many molecules: small molecules,[24] transition metal compounds,[25] porphine,[26] fullerenes.[27] Although some questions are still open from a methodological point of view, these studies underline the interest of this method and also its limits. In particular, the excited states must be mainly described by single excitations. This important restriction of TD-DFT methods excludes its application to multielectron excitation phenomena, which, however, do not occur in the present study.

Experimental

Chemicals

Ethanol (95%) and isopentane were obtained from Aldrich. Ketoprofen [2-(3-benzoylphenyl)propionic acid] was purchased from Specia, fenofibrate {2-[4-(4-chlorobenzoyl) phenoxy]-2-methylpropanoic acid 1-methylethyl ester} from Sigma, and benzophenone from Fluka; all were used as received without purification. Fenofibric acid was obtained by saponification of fenofibrate by NaOH, followed by precipitation in the presence of H_2SO_4.

Absorption and emission spectra and lifetime measurements

The ultraviolet absorption spectra were measured in ethanol, isopentane and 5 mM phosphate buffer containing 10 mM NaCl at pH 7.4 by means of an HP 8452A diode array spectrophotometer.

Emission and excitation spectra were obtained on a Perkin Elmer LS-50B spectrofluorimeter equipped with a xenon source (flash duration 8 μs) and a Hamamatsu R928 photomultiplier tube with the low temperature accessory L2250136. The apparatus was operated in time-resolved mode, with a delay time of 0.1 ms and a gate of 5 ms. Excitation and emission monochromator band passes of 5 nm were used. The sample was put in a capillary tube (2 mm in diameter) and cooled to 77 K in a liquid nitrogen bath. Dry nitrogen circulation in the cell compartment avoided water condensation on the cell walls. The emission was obtained by exciting the samples at 313 nm in different media, using an absorbance of about 0.05 in a 10 mm cell. Phosphorescence lifetimes (τ) were obtained by time-resolved detection of the emission intensity at the emission maximum wavelength. The emission decay curves were fitted to an equation of the form $I(t) = I_0 \exp(-t/\tau)$ using a non-linear least squares minimisation algorithm. High correlation coefficients (0.999) were obtained in all cases.

Laser flash photolysis

Transient absorption spectra and excited state lifetimes were determined by laser flash spectroscopy using a set up described elsewhere in detail.[28] Briefly, an excimer laser (Lambda Physik EMG 100, 308 nm, 10 ns pulses of 150 mJ) was used as an excitation source. The detection system consisted of a xenon flash lamp, a Jobin Yvon H25 monochromator, a Hamamatsu R955 photomultiplier and a Le Croy 9362 digital oscilloscope. The laser intensity was attenuated to avoid biphotonic effects.

The measurements were performed at room temperature. The analysis was carried out within the first millimeters of the sample excited by the laser pulse, using quartz cells of 10 mm path length. The concentration of the ethanol solutions (5×10^{-5} M) was such that the optical density was around 0.8 at the excitation wavelength of the laser. Solutions were deaerated by bubbling for 15 min with argon before experimentation.

Quantum mechanical methodology

We used the time-dependent local density approximation theory (TD-LDA). Although Casida *et al.*[24] demonstrated that TD-LDA does remarkably well for low-lying excited states with valence character, recent studies have shown that hybrid functionals (*e.g.*, B3LYP), functionals having the correct asymptotic behaviour (*e.g.*, HCTH[29]), or generalised gradient approximation functionals (*e.g.*, PBE0[30]) may improve the theoretical spectra. However, while B3LYP is far more time-consuming than TD-LDA, PBE0 has not yet been implemented in commercial quantum chemistry packages. These states must lie below the LDA ionisation threshold, that is, the negative of the energy of the highest occupied MO ($-\varepsilon_{HOMO}^{LDA}$).

The wavefunction Ψ_I for the Ith excited state has the form[24]

$$\Psi_I = \sum_{i \in \text{occ}} \sum_{j \in \text{virt}} C_{ij}^I \Phi_{i \to j}$$

where $\Phi_{i \to j}$ is the determinant representing an excitation from the occupied $MO_{\varphi i}$ towards the virtual $MO_{\varphi j}$ and C_{ij}^I is the weight of that determinant in the wavefunction Ψ_I. Thus, the analysis of the nature of the states is supported by the values of the C_{ij}^I coefficients in the TD-LDA wavefunction and by the shapes of the LDA MOs.

We assume that the DFT MOs are suitable for a good description of the electronic structure of molecules, as Hartree–Fock or extended Hückel MOs. This is in particular suggested by work in the groups of Baerends,[31] Hoffmann[32] and Salahub.[33]

All the calculations were performed with the GAUSSIAN 98 quantum chemistry program.[34] We used energy adapted pseudopotentials for the inner core electrons,[35] and double zeta basis sets to describe the valence electrons. We added a d polarisation function on carbon ($\zeta_d = 0.75$), oxygen ($\zeta_d = 0.85$) and chloride ($\zeta_d = 0.65$). We have checked that adding diffuse functions on C and O does not significantly improve the vertical transition energies of BP. The geometries were optimised at the DFT level of theory. We used the Becke–Perdew functional (BP86) for BP and KP, while FB was optimised with the LDA functional. In all cases, the excited states were calculated with the TD-LDA method (SVWN5 functional) for the optimal geometry in the ground electronic state. We computed the energies and wavefunctions of 10 singlet and 10 triplet states above the ground state. We also computed the oscillator strengths for singlet states in order to compare with experimental intensities. Geometry optimisations as well as excited state calculations were performed on isolated molecules.

Results and discussion

UV absorption spectra

The UV absorption spectrum of KP in 5 mM phosphate buffer containing 10 mM NaCl at pH 7.4 is characterised by an intense band at 260 nm ($\varepsilon_{max} = 16\,000$ M^{-1} cm^{-1}), which undergoes the bathochromic shift characteristic of a $\pi\pi^*$

orbital transition when the solvent polarity is decreased (λ_{max} shifts to 256 and 248 nm in ethanol and isopentane, respectively) as shown in Fig. 1(*A*). In contrast, an $n\pi^*$ band of lower intensity appearing at 332 nm ($\varepsilon_{max} = 150\ M^{-1}\ cm^{-1}$) in ethanol shifted to the red ($\lambda = 346$ nm) in isopentane [Fig. 1(*A*) insert] but was not observed in buffer solution. These spectral characteristics are nearly the same as those of benzophenone, which exhibits two bands located at 254 and 332 nm in ethanol[36,37] and at 248 and 346 nm in isopentane. In isopentane, KP also displayed a new band of low intensity in the 280–300 nm region, corresponding to a second $\pi\pi^*$ transition due to the dissymmetric structure of this benzophenone derivative. In polar solvent, this band was not observed: it may well be hidden by the first $\pi\pi^*$ band of higher intensity.

The absorption spectrum of FB is significantly different from that of KP [Fig. 1(*B*)]. FB absorbs at higher wavelengths than KP. The main band is located at 298 nm in phosphate buffer. While it does not show any significant shift when changing solvent from phosphate buffer to ethanol or isopentane (294 nm), its high absorbance ($\varepsilon_{max} = 15\,000\ M^{-1}\ cm^{-1}$ in buffer) led us to assign a preponderant $\pi\pi^*$ character to this transition. A second $\pi\pi^*$ transition, found at 272 nm in phosphate buffer and moving to 258 nm in ethanol and to 256 nm in isopentane, was also observed for FB. The difference in the relative intensity of the two $\pi\pi^*$ bands observed in the KP and FB spectrum is very likely due to the presence of the *O*-alkyl substituent in the case of FB. It is known that the presence of an electron-donating group has little affect on the $\pi\pi^*$ band near 260 nm but induces a strong absorption at longer wavelengths.[38] No $n\pi^*$ band was detected in the spectrum of FB in any solvent but one might be hidden in the tail of the $\pi\pi^*$ band, as reported for similarly substituted ketones.[39]

Phosphorescence spectra

The phosphorescence emission spectrum of KP and FB were measured at 77 K in the same solvents as those used for the absorption spectra. KP shows in ethanol and isopentane an emission spectrum identical to that of benzophenone. In ethanol glass, the phosphorescence emission spectrum, obtained by excitation of KP at 313 nm, exhibits a fingered pattern of vibrational structure with a maximum at 445 nm [Fig. 2(*A*)]. The spacing between vibronic bands in the vibrational structure of the phosphorescence spectrum is 1600 cm^{-1}. The triplet lifetime measured by following the decay of the emission at 445 nm after laser excitation at 313 nm is 6 ms. The triplet energy evaluated from the 0-0 band of the emission spectrum (415 nm) is 69.3 kcal mol^{-1}. On the basis of the triplet lifetime and spacing between vibronic bands, the lowest triplet state of KP was assigned to an $n\pi^*$ triplet state, as for BP. The excitation spectrum corresponding to an emission at 445 nm was then recorded from the same sample at 77 K. The energy of the lowest $n\pi^*$ singlet excited state, 77.3 kcal mol^{-1}, was calculated from the 0-0 band of the excitation spectrum at 371 nm [Fig. 2(*A*)]. The singlet-triplet splitting was found to be equal to 2400 cm^{-1}. When changing solvent from ethanol to isopentane, the KP phosphorescence spectrum was shifted to the red by 10 nm while in phosphate buffer, the less well resolved spectrum underwent a hypsochromic shift of 5 nm.

The phosphorescence emission spectrum of FB under the same conditions [Fig. 2(*B*)] displays a vibrational structure with a pattern very similar to those of BP and KP with an emission maximum at 451 nm in ethanol and a 1500 cm^{-1} spacing between the vibronic bands of the phosphorescence spectrum, which is characteristic of a carbonyl stretching and is in agreement with an $n\pi^*$ state. As expected, the triplet lifetime was not strongly modified by the presence of an *O*-alkyl group.[40] It was of the same order of magnitude as that of KP or BP ($\tau = 9$ ms). This set of features shows that the lowest excited state of FB is an $n\pi^*$ triplet state. The energy of this triplet state was found to be equal to 68.1 kcal mol^{-1} (421 nm). It is slightly lower than that of KP or BP. The phosphorescence spectrum, as well as the excitation spectrum recorded for an emission wavelength of 451 nm [Fig. 2(*B*)], were not modified on using phosphate buffer or isopentane in place of ethanol.

From this spectroscopic study it appears that while both FB and KP have BP-like structures, their singlet-singlet transitions are different. Due to the presence of an *O*-alkyl substituent in FB, two well defined singlet $\pi\pi^*$ excited states are

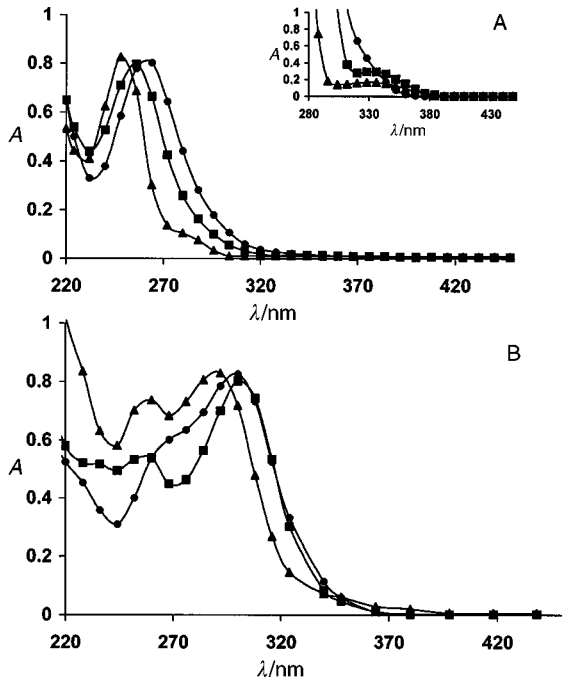

Fig. 1 UV-visible absorption spectra of (*A*) KP and (*B*) FB in different solvents: (●) phosphate buffer; (■) ethanol, (▲) isopentane. Drug concentration: 5×10^{-5} M. Inset: drug concentration: 2×10^{-3} M.

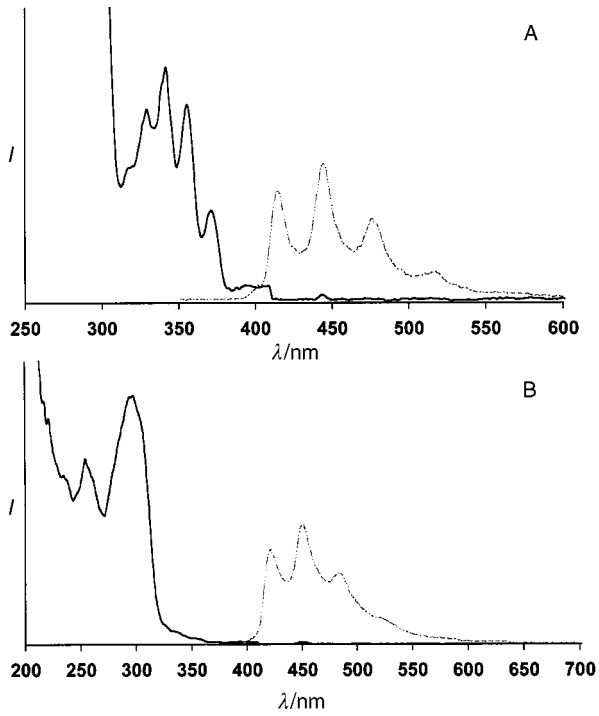

Fig. 2 (*A*) Phosphorescence emission (dashed line) and excitation (full line) spectra of KP in ethanol at 77 K. (*B*) Phosphorescence emission (dashed line) and excitation (full line) spectra of FB in ethanol at 77 K.

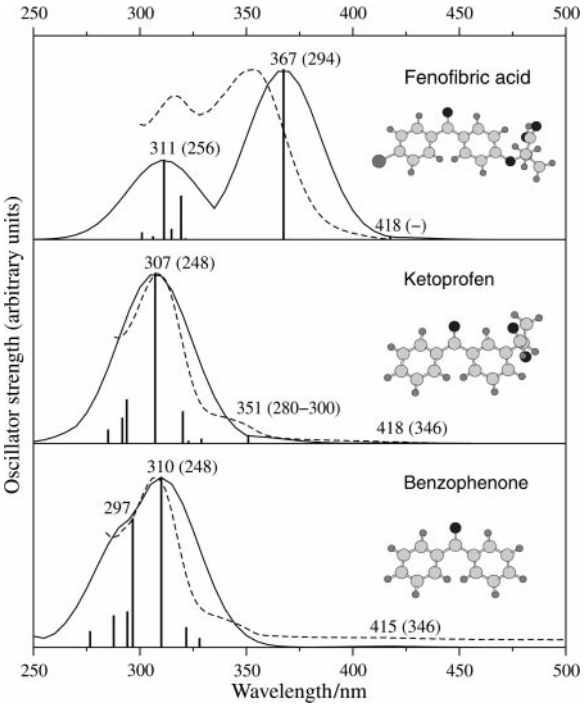

Fig. 3 TD-LDA calculated absorption wavelengths and oscillator strengths with the optimised geometries of BP, KP, and FB. Superimposed is the shifted experimental UV spectrum (dashed curves). The theoretical transitions are convoluted with Gaussian-type functions (full curves). The values in parentheses correspond to the experimental wavelengths given in Table 1.

found. The expected $n\pi^*$ singlet excited state is not detected in the spectrum of FB but may be hidden by the new $\pi\pi^*$ band. In contrast, the lowest triplet excited state is seen to be of $n\pi^*$ type in both cases. To support these assignments, theoretical calculations have been performed by the TD-DFT method.

Theoretical calculations

The wavelengths and the oscillator strengths corresponding to the vertical transitions from the ground state to the lowest singlet excited states for the UV absorption spectra in isopentane, as well as the optimised geometries of BP, KP and FB, are reported in Fig. 3. As can be seen, these molecules are not planar, due to the important steric repulsion between H atoms. BP has C_2 symmetry and a torsion angle $\tau = 30.3°$, which compares very well with the value deduced from free-jet absorption millimeter-wave experiments ($\tau = 31.7°$).[41] The angle between the phenyl planes is equal to 52° for BP, a value also in very good agreement with that found by different experimental techniques[41,42] and is 52° for KP and 46° for FB. For the purpose of comparison with experimental spectra, the peaks were convoluted with Gaussian-type functions, as usually done to qualitatively reproduce the experimental band width. The shape of the Gaussian functions is chosen to take into account the vibrational motions of the atoms.

The theoretical absorption spectra of BP, KP and FB present similar features: a weak transition around 415 nm and an intense band around 310 nm. Two singlet states display a large oscillator strength for BP, which leads to a shoulder in the band at 310 nm. We checked that this shoulder vanishes with a slight modification of the geometry, such as the angle between the phenyl groups. In the case of FB, the most intense transition occurs at 367 nm. This is due to a transition towards a unique excited state, while the energy bands at 310 nm correspond to the absorption of many states, as can be seen from Fig. 3. It is interesting to notice that the absorption of the lowest S_2 state is not necessarily the most intense, hence the necessity to calculate several singlet states.

The main features of the theoretical spectra are consistent with the experimental ones, although there is a systematic red shift with respect to experiment. The average deviation from the absorption spectrum obtained in a non-polar solvent (isopentane) is approximately 60 nm, which corresponds to an energy difference of a few kcal mol^{-1} in this wavelength range. Thus, the experimental data reported in Fig. 3 (dashed lines) were shifted to facilitate the comparison with the theoretical results. This uniform offset is justified by the very good fit between "shifted experiment" and theory. This good agreement validates the application of the TD-LDA method to such molecules and allows the use of almost the same offset to deal with the triplet states. A similar shift was applied, for example, in ref. 27, in which a theoretical justification of the discrepancy between experimental and TD-DFT calculations is given.

Table 1 Vertical transition wavelengths (in nm) calculated at different levels of theory

State[a]	Method		BP	KP	FB
$S_1(n,\pi^*)$	Expt	λ_{max}	346[b]	346[b]	Not obsd
	CNDO/S[c]	λ	378	360	Not calcd
	TD-LDA	λ	415	418	418
		Ψ	$0.65(n \rightarrow \pi_1^*)$	$0.65(n \rightarrow \pi_1^*)$	$0.62(n \rightarrow \pi_1^*)$
$S_2(\pi,\pi^*)$	Expt	λ_{max}	—	—	294[d]
	TD-LDA	λ	—	—	367
		Ψ	—	—	$0.59(\pi_2 \rightarrow \pi_1^*)$
$S_k(\pi,\pi^*)$	Expt	λ_{max}	248[b]	248[b]	256[d]
	TD-LDA	λ	310	307	311
		Ψ	$0.45(\pi_1 \rightarrow \pi_1^*)$	$0.43(\pi_2 \rightarrow \pi_1^*)$	$0.51(n \rightarrow \pi_2^*)$
			$0.34(\pi_3 \rightarrow \pi_1^*)$	$0.35(\pi_1 \rightarrow \pi_1^*)$	$0.36(\pi_1 \rightarrow \pi_1^*)$
			$0.34(n \rightarrow \pi_2^*)$	Other[e]	
$T_1(n,\pi^*)$	Expt	λ_{00}	421	423.5[b]	423.5[d]
	CNDO/S[f]	λ	401	402	Not calcd
	TD-LDA	λ	482	487	489
		Ψ	$0.76(n \rightarrow \pi_1^*)$	$0.76(n \rightarrow \pi_1^*)$	$0.76(n \rightarrow \pi_1^*)$
$T_2(\pi,\pi^*)$	CNDO/S[f]	λ	394	394	Not calcd
	TD-LDA	λ	369	377	431
		Ψ	$0.76(\pi_2 \rightarrow \pi_1^*)$	$0.61(\pi_4 \rightarrow \pi_1^*)$	$0.74(\pi_2 \rightarrow \pi_1^*)$

Experimental λ_{max} are given for comparison. For the present TD-LDA calculations, the main determinants defining the wavefunctions are also given. [a] States are numbered according to their theoretical relative ordering. The $S_2(\pi,\pi^*)$ states of BP and KP do not have significant oscillator strength and therefore are not given in this table. S_k refers to the most intense π,π^* state ($k = 4$, 6, 7 for BP, KP and FB, respectively). [b] In isopentane. [c] From ref. 17, with solvent effect. [d] In 10% ethanol–90% isopentane. [e] There are also significant contributions of excitations from π_2, π_3 and n towards π_2^* and π_3^*. [f] From ref. 17, in gas phase.

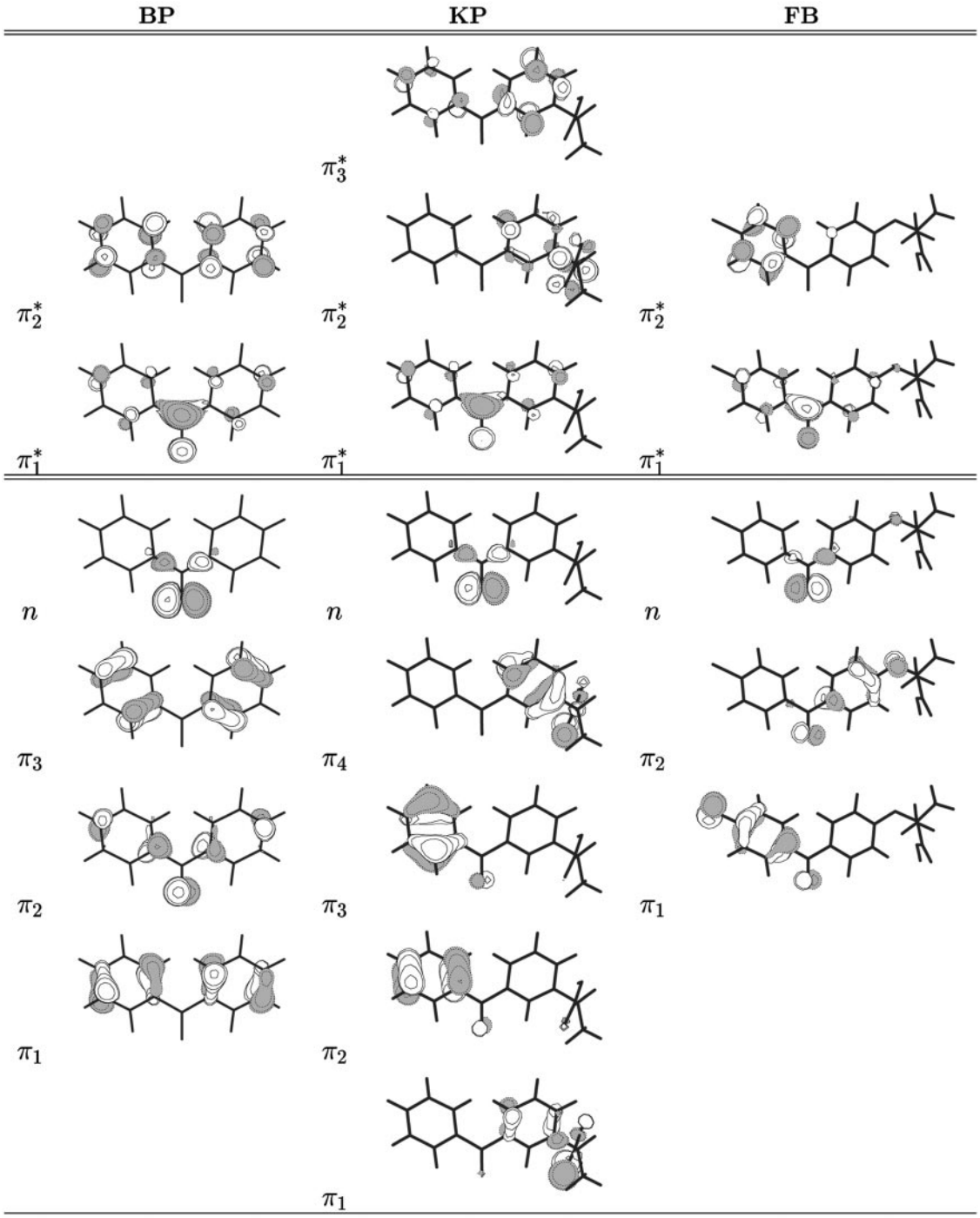

Fig. 4 Highest occupied and lowest unoccupied LDA orbitals from which the TD-LDA wavefunctions are defined.

The analysis of the character of some wavefunctions (ψ) is reported in Table 1, as well as the wavelengths found in the above experiments and in previous semi-empirical CNDO/S calculations.[17] The highest occupied and lowest unoccupied MOs of the three molecules are shown in Fig. 4. In all cases, the HOMO is a lone pair (*n*) on the oxygen of the carbonyl group, while the LUMO is a π^* orbital localised on the carbonyl group with tails on the phenyl groups.

We identify the lowest singlet and triplet states of BP, KP and FB as having mainly $n\pi^*$ character [$S_1 \sim 0.65$ ($n\pi^*_{LUMO}$) and $T_1 \sim 0.76$ ($n\pi^*_{LUMO}$), see Table 1], while the higher states have a $\pi\pi^*$ character. Although the experimental absorption spectrum of FB does not reveal the presence of an $n\pi^*$ state, the present calculations suggest it exists and that is hidden in the foot of the first $\pi\pi^*$ band (see Fig. 3). From the theoretical results, this $\pi\pi^*$ band, not observed for BP and KP, and which corresponds to high absorption, is due to a unique state essentially described by excitation from a π orbital localised on the phenyl group bearing the *O*-alkyl substituent towards the LUMO. The chlorine atom does not participate in the description of this state.

A state energy diagram for BP, KP and FB can be deduced from the present TD-LDA calculations. The vertical energies (in kcal mol^{-1}) of the lowest singlet and triplet states, as well as the singlet that exhibits the highest oscillator strength, are reported in Fig. 5. These are the most relevant excited states according to the interpretation of experimental results. All these states lie far below the ionisation threshold ($-\varepsilon^{LDA}_{HOMO}$ is approximately 130 kcal mol^{-1} for the three benzophenone derivatives). In the case of FB, a triplet $\pi\pi^*$ state, T_2 corresponding to the same transition ($\pi_2 \rightarrow \pi_1^*$) as the singlet S_2 state (Table 1), appears 8 kcal mol^{-1} above the $T_1(n\pi^*)$ state while for BP and KP, the first $^3\pi\pi^*$ state, $T_2(\pi\pi^*)$, is approximately 17 kcal mol^{-1} above T_1. The state energy diagram of

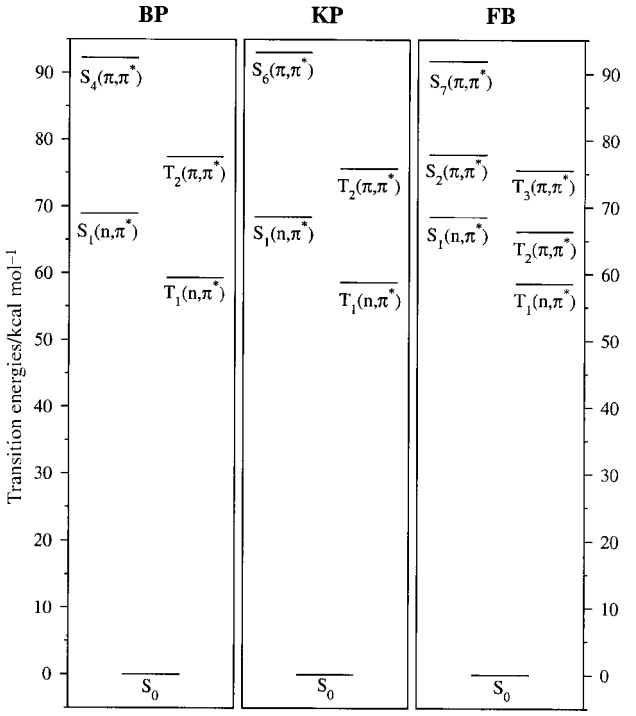

Fig. 5 State energy diagram of the lowest singlet and triplets states, as well as the singlet states which have the most intense absorptions. The energies are vertical transition energies from the ground state S_0. For a quantitative agreement with experimental data, they should be shifted by approximately +5 kcal mol^{-1}.

these compounds is in agreement with that previously given for BP, which exhibits a $S_1(n\pi^*)$ close in energy to two triplet states $T(n\pi^*)$ and $T(\pi\pi^*)$.[36] The energies of $S_1(n\pi^*)$ and $T_1(n\pi^*)$ calculated for BP are in agreement with the experimental values determined by spectroscopy already reported in the literature.[36] The $T_2(\pi\pi^*)$ energy level of BP is not so well established. The high quantum yield of phosphorescence of BP is consistent with an efficient intersystem crossing occurring *via* spin-orbit coupling from $S_1(n\pi^*)$ to $T_2(\pi\pi^*)$, followed by rapid internal conversion from $T_2(\pi\pi^*)$ to $T_1(n\pi^*)$. However, the relative positions of $S_1(n\pi^*)$ and $T_2(\pi\pi^*)$ has been a controversial subject for some years. Early on, around 1960–1970, photochemists correlated the large rate constant of intersystem crossing in BP ($\sim 10^{11}$ s^{-1})[21] to the presence of a $T_2(\pi\pi^*)$ state slightly below (a few kcal mol^{-1})[19] $S_1(n\pi^*)$. Some years later, different experiments led to the conclusion that $T_2(\pi\pi^*)$ may, in fact, lie higher than $S_1(n\pi^*)$, the $S_1(n\pi^*) - T_2(\pi\pi^*)$ energy gap being, however, very small.[43–45] The present TD-LDA results provide a similar ordering while the S_1-T_2 energy gap, around 9 kcal mol^{-1}, may be slightly overestimated.

In contrast, there is a discrepancy between our results, concerning in particular the large energy difference between the two lowest triplet states, and those found by previous CNDO/S calculations[17] on BP and KP in the gas phase. The latter method provides two almost degenerate states, and the analysis of the lowest triplet states indicates an $n\pi^*$ character for BP and a more pronounced $\pi\pi^*$ character for KP. The same characterisation was obtained for the lowest singlet excited states of BP and KP, while UV experiments show that this state is $n\pi^*$ in any solvent. Thus, unlike TD-LDA results, CNDO/S singlet wavefunctions do not seem to be fully consistent with the experimental observations, though the CNDO/S energies of $S_1(n\pi^*)$ are in fair agreement with UV absorption spectra (see Table 1).

Laser flash photolysis experiments

In a parallel approach, nanosecond laser flash photolysis experiments were carried out to obtain further information on the characterstics of the triplet state of FB by comparison with those of BP or KP. The transient absorption changes of fenofibric acid and its isopropyl ester, which does not give rise to a photodecarboxylation process, have been determined in argon-saturated ethanol solutions. The difference absorption spectra of fenofibrate observed 40 or 400 ns after the laser pulse are shown on Fig. 6(*A*). After 40 ns the transient absorbance spectrum was characterised by two positive bands: a UV band with two sharp peaks at 325 nm and 345 nm and a visible broad band with maxima at 520 and 550 nm. This visible band disappeared by a first-order process (τ = 225 ns) with the simultaneous growth of the UV band at the same rate (235 ns) to give a long-lived transient. Its absorption spectrum observed at 400 ns is similar to the spectrum observed at 40 ns, but the relative intensities of the UV peaks are inverted, the absorption at 345 nm becoming the main peak. In aerated solutions, the transient absorption decays by a first order process (τ = 205 ns). The photochemical behaviour in degassed or non-degassed solutions is reminiscent of that observed in flush photolysis studies of BP or KP.

The absorption spectrum and lifetime of the lowest excited state of benzophenone has been extensively studied in different solvents.[46] In ethanol, flash photolysis produced a strong absorption with maxima at 315 and 525 nm for the triplet state,[47] as in water,[48] and a weaker absorption with maximum at 330 and 545 nm for the ketyl radical in ethanol[47] (540 nm in water[49]). Time-resolved results obtained by Martinez and Scaiano in solvents other than water show that KP (or KP ethyl ester) triplet absorbs with maxima at 320 and 520 nm[18] (526 nm in water[17]). Addition of an H-atom donating compound led to absorption at 330 and 545 nm, indicative of the generation of ketyl radicals. Thus, by comparison to BP or KP, it may be assumed that the transient spectra observed

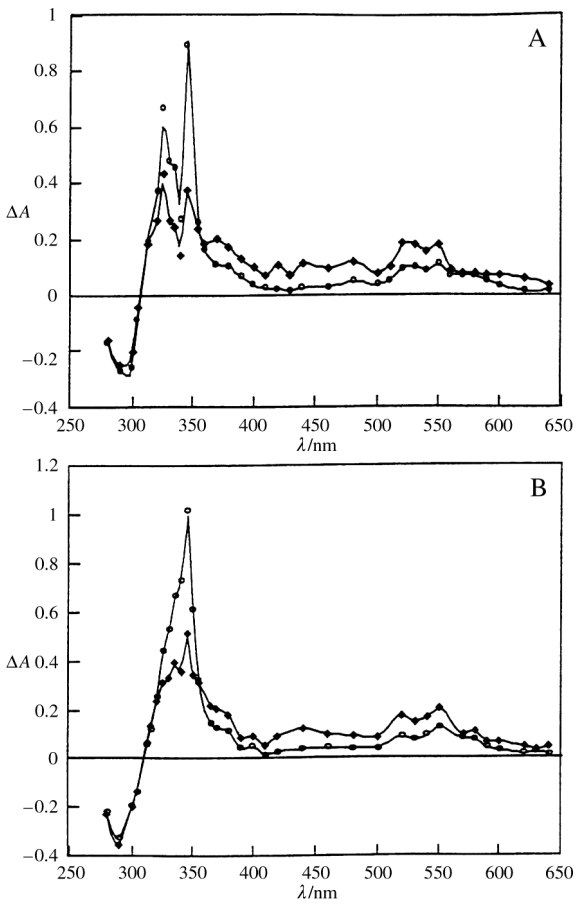

Fig. 6 Transient absorption spectra obtained from the 308 nm laser flash photolysis of (*A*) fenofibrate and (*B*) fenofibric acid in ethanol: (◆) 40 and (○) 400 ns after the laser pulse.

for fenofibrate correspond to a triplet-triplet absorption at 325 and 520 nm with a contribution from the ketyl radical absorption at 345 and 550 nm.

The behaviour of FB in degassed ethanolic solution under laser flash photolysis resembles that of its ester derivative [Fig. 6(*B*)]. The spectral shape of the transients observed after 40 ns shows a maximum at 345 nm and a band of lower intensity with maxima at 520 and 550 nm. By analogy to fenofibrate, ketoprofen and benzophenone, the maxima at 550 nm may be attributed to the ketyl radical of FB due to a reductive process. The maxima at 520 nm may be attributed to a contribution of the triplet state similar to that of fenofibrate. The triplet state decays by a first order process (335 ns) to give the ketyl radical at the same rate (365 ns). In aerated solutions, the decay of the triplet state only (225 ns) was observed. An estimate for the rate constant of the quenching of the FB triplet state by oxygen leads to a value of 6.9×10^8 M^{-1} $s,^{-1}$ similar to that reported for the quenching of the benzophenone triplet state by oxygen (4×10^8 M^{-1} s^{-1} [49]). As in the case of KP and its ethyl ester, the transient intermediates observed for FB and FB isopropyl ester have the same spectral features characteristic of transients arising from the benzophenone moiety.

These laser flash experiments show the formation of a ketyl radical during the irradiation of both FB and its ester derivative in alcoholic solution, the radical being produced from the triplet state by H-abstraction from the solvent. Such a behaviour is typical of the $n\pi^*$ triplet of aromatic ketones. This is consistent with the nature of the photoproducts obtained in methanol solution of such compounds. In the case of BP, it has been demonstrated that according to the conditions (presence or absence of oxygen, ketone concentration) the ketyl radical so formed may either dimerise or recombine with the radical formed from the solvent, to give the benzopinacol or a tertiary alcohol, respectively.[36] These reactions characteristic of the ketyl radical were observed in the photolysis of KP in methanol, which is converted to a large extent to the corresponding benzopinacol,[11] and in the photodegradation of FB isopropyl ester, which gave rise under anaerobic conditions to two photoproducts, one resulting from the dimerisation of the ketyl radical, the second one from the recombination of the ketyl radical with the alkyl radical formed on the solvent.[12]

Conclusion

Low temperature spectroscopy has clearly shown that although the three benzophenone derivatives investigated are differently substituted, their lowest triplet state in all cases was an $n\pi^*$ triplet state. Theoretical TD-LDA calculations agree fairly well with the description of the excited states on the basis of the spectroscopic study. To our knowledge, the only previously available theoretical results were obtained for BP and KP at the CNDO/S level of calculation.[17] The TD-LDA results disagree with the analysis of the nature of S_1 and T_1 of BP and KP provided by CNDO/S, while they seem to be in better agreement with most of the experimental data reported here. Indeed, they clearly point out that the lowest singlet and triplet states have $n\pi^*$ character in all the benzophenone derivatives studied. Calculations with more accurate methods are in progress and appear to lead to the same conclusion. Of course, state energy diagrams only give a rough picture of the complex mechanisms of photochemical reactions, and exploration of the ground and excited state potential energy surfaces are necessary to understand these mechanisms.[50] The present TD-LDA work should be considered as a preliminary step towards more comprehensive studies. These results are supported by flash photolysis experiments in alcoholic solutions, pointing to a hydrogen abstraction reaction characteristic of a carbonyl group in its $n\pi^*$ triplet state. The formation of a ketyl radical in a hydrogen-donating medium may explain the ability of these compounds to induce *in vivo* radical processes such as lipid peroxidation or crosslinking involved, respectively, in phototoxic or photoallergic effects. The decarboxylation processes that occur in phosphate buffer and involve the carboxylate of FB or KP required more complex calculations on the different states of these anionic forms. New studies are currently in progress to account for the reactivity of FB and KP in water.

Acknowledgements

The authors thank Dr. Mark Casida and Dr. Franck Jolibois for helpful discussions and for their interest in the theoretical part of this work. They are also indebted to Dr Claude Picard for access to the spectrofluorometer and kind advice in the achievement of low temperature experiments.

References

1 A. Albani and E. Fasani, *Drugs, Photochemistry and Photostability*, Royal Society of Chemistry, Cambridge, 1998.
2 F. Bosca and M. A. Miranda, *J. Photochem. Photobiol. B*, 1998, **43**, 1.
3 G. Dorman and G. Prestwich, *Biochemistry*, 1994, **33**, 5661.
4 G. Serrano, J. M. Fortea, J. M. Latasa, F. Millan, C. Janes, F. Bosca and M. A. Miranda, *J. Am. Acad. Dermatol.*, 1992, **27**, 204.
5 M. C. Marguery, F. El Sayed, J. Rakotondrazafy, R. Saqi, G. Samalens, B. Gorguet and J. Bazex, *Eur. J. Dermatol.*, 1995, **5**, 204.
6 A. Alomar, *Contact Dermatitis*, 1985, **12**, 112.
7 F. Cusano, B. R. Rafenelli, R. Bacchilega and G. Errico, *Contact Dermatitis*, 1987, **21**, 108.
8 N. Mozzanica and P. D. Piggatto, *Contact Dermatitis*, 1990, **23**, 336.
9 R. T. Nabeja, T. Kojima and M. Fujita, *Contact Dermatitis*, 1995, **32**, 52.
10 D. Leroy, A. Dompmartin, E. Lorler, Y. Leport and C. Audebert, *Photodermatol. Photoimmunol. Photomed.*, 1990, **7**, 136.
11 F. Bosca, M. A. Miranda, G. Carganico and D. Mauleon, *Photochem. Photobiol.*, 1994, **60**, 96.
12 F. Vargas, N. Canudas, M. A. Miranda and F. Bosca, *Photochem. Photobiol.*, 1993, **58**, 471.
13 P. Pietta, E. Manera and P. Ceva, *J. Chromatogr.*, 1987, **390**, 454.
14 L. L Costanzo, G. de Guidi, G. Condorelli, A. Cambria and M. Fama, *Photochem. Photobiol.*, 1989, **50**, 359.
15 M. A. Miranda, F. Bosca, F. Vargas and N. Canudas, *Photochem. Photobiol.*, 1994, **59**, 171.
16 M.-C. Marguery, N. Chouini–Lalanne, J.-C. Ader and N. Paillous, *Photochem. Photobiol.*, 1998, **68**, 679.
17 S. Monti, S. Sortino, G. De Guidi and G. Marconi, *J. Chem. Soc., Faraday Trans.*, 1997, **93**, 2269.
18 L. J. Martinez and J. C. Scaiano, *J. Am. Chem. Soc.*, 1997, **119**, 11066.
19 M. A. El-Sayed, *Acc. Chem. Res.*, 1968, **1**, 8.
20 M. A. El-Sayed and R. Leyerle, *J. Chem. Phys.*, 1975, **62**, 1579.
21 R. M. Hochstrasser, *Acc. Chem. Res.*, 1968, **1**, 266.
22 B. O. Roos, *Acc. Chem. Res.*, 1999, **32**, 137.
23 M. E. Casida, in *Recent Developments and Applications of Modern Density Functional Theory*, ed. J. M. Seminario, Elsevier Science, Amsterdam, 1996; K. Burke and E. K. U. Gross, in *Density Functionals: Theory and Applications*, ed. D. Joubert, Springer, Berlin, 1998, p. 116.
24 M. E. Casida, C. Jamorski, K. C. Casida and D. R. Salahub, *J. Chem. Phys.*, 1998, **108**, 4439.
25 S. J. A. van Gisbergen, J. A. Groeneveld, A. Rosa, J. G. Sniders and E. J. Baerends, *J. Phys. Chem.*, 1999, **103**, 6835.
26 S. J. A. van Gisbergen, A. Rosa, G. Ricciardi and E. J. Baerends, *J. Chem. Phys.*, 1999, **111**, 2499.
27 R. Bauernschmitt, R. Ahlrichs, F. K. Hennrich and M. M. Kappes, *J. Am .Chem. Soc.*, 1998, **120**, 5052.
28 E. Amouyal and M. Mouallem–Bahout, *J. Chem. Soc., Dalton Trans.*, 1992, 509.
29 D. J. Tozer and N. C. Handy, *J. Chem. Phys.*, 1998, **109**, 10180.
30 C. Adamo, G. E. Scuseria and V. Barone, *J. Chem. Phys.*, 1999, **111**, 2889.

31 E. J. Baerends, O. V. Gritsenko and R. van Leeuwen, *ACS Symp. Ser.*, 1996, **629**, 20.
32 R. Stowasser and R. Hoffmann, *J. Am. Chem. Soc.*, 1999, **121**, 3414.
33 P. Duffy, D. P. Chong, M. E. Casida and D. R. Salahub, *Phys. Rev. A*, 1994, **50**, 4707.
34 M. J. Frisch, G. W. Trucks, H. B. Schlegel, G. E. Scuseria, M. A. Robb, J. R. Cheeseman, V. G. Zakrzewski, J. A. Montgomery, R. E. Stratmann, J. C. Burant, S. Dapprich, J. M. Millam, A. D. Daniels, K. N. Kudin, M. C. Strain, O. Farkas, J. Tomasi, V. Barone, M. Cossi, R. Cammi, B. Mennucci, C. Pomeli, C. Adamo, S. Clifford, J. Ochterski, G. A. Petersson, P. Y. Ayala, Q. Cui, K. Mokoruma, D. K. Malick, A. D. Rabuck, K. Raghavachari, J. B. Foresman, J. Cioslowski, J. V. Ortiz, B. B. Stefanov, G. Liu, A. Liashenko, P. Piskorz, I. Komaromi, R. Gomperts, R. L. Martin, D. J. Fox, T. Keith, M. A. Al-Laham, C. Y. Peng, A. Nanayakkara, C. Gonzalez, M. Challacombe, P. M. W. Gill, B. G. Johnson, W. Chen, M. W. Wong, J. L. Andres, M. Head–Gordon, E. S. Replogle and J. A. Pople, *GAUSSIAN 98*, Gaussian, Inc., Pittsburgh PA, 1998.
35 A. Bergner, M. Dolg, W. Kuechle, H. Stoll and H. Preuss, *Mol. Phys.*, 1993, **80**, 1431.
36 N. J. Turro, *Modern Molecular Photochemistry*, University Science Books, Mill Valley, CA, 1991.
37 P. Suppan, *Chemistry and Light*, Royal Society of Chemistry, Cambridge, 1994.
38 G. Porter and P. Suppan, *Trans. Faraday Soc.*, 1965, **61**, 1664.
39 P. J. Wagner, A. E. Kemppainen and and H. N. Schott, *J. Am. Chem. Soc.*, 1973, **95**, 5604.
40 P. J. Wagner, R. J. Truman and J. C. Scaiano, *J. Am. Chem. Soc.*, 1985, **107**, 7093.
41 E. B. Fleisher, N. Sung and S. Hawkinson, *J. Phys. Chem.*, 1968, **72**, 4311.
42 A. Maris, S. Melandri, W. Caminati and P. G. Favero, *Chem. Phys. Lett.*, 1996, **256**, 509.
43 M. Batley and D. R. Kearns, *Chem. Phys. Lett.*, 1968, **2**, 423.
44 J. M. Morris and D. F. Willams, *Chem. Phys. Lett.*, 1974, **25**, 312.
45 N. Ohmori, T. Suzuki and M. Ito, *J. Phys. Chem.*, 1988, **92**, 1086.
46 I. Carmichael and G. L. Hug, *J. Phys. Chem. Ref. Data*, 1986, **15**, 55.
47 Y. I. Kiryukhin, Z. A. Sinitsyna and K. S. Bagdasar'yan., *High Energy Chem.*, 1979, **13**, 432.
48 R. V. Bensasson and J.-C. Gramain, *J. Chem. Soc. Faraday Trans. 1*, 1980, **76**, 1801.
49 M. B. Ledger and G. Porter, *J. Chem. Soc. Faraday Trans. 1*, 1972, **68**, 539.
50 F. Bernadi, M. Olivucci and M. A. Robb, *Chem. Soc. Rev.*, 1996, **25**, 321 and references therein.